

On the Encounter Desorption of Hydrogen Atoms on Ice Mantle

Qiang Chang¹, Xuli Zheng², Xia Zhang², Donghui Quan^{2,3}, Yang Lu⁴, Qingkuan Meng¹,
Xiaohu Li² and Long-Fei Chen²

¹ School of Physics and Optoelectronic Engineering, Shandong University of Technology, Zibo, 255000, China; changqiang@sdut.edu.cn

² Xinjiang Astronomical Observatory, Chinese Academy of Sciences, 150 Science 1-Street, Urumqi 830011, PR China; zhangx@xao.ac.cn

³ Department of Chemistry, Eastern Kentucky University, Richmond, KY 40475, USA

⁴ School of Physics & Astronomy, Sun Yat-Sen University, Zhuhai 519082, China

Received 20xx month day; accepted 20xx month day

Abstract At low temperatures (~ 10 K), hydrogen atoms can diffuse quickly on grain ice mantles and frequently encounter hydrogen molecules, which cover a notable fraction of grain surface. The desorption energy of H atoms on H₂ substrates is much less than that on water ice. The H atom encounter desorption mechanism is adopted to study the enhanced desorption of H atoms on H₂ substrates. Using a small reaction network, we show that the steady-state surface H abundances predicted by the rate equation model that includes H atom encounter desorption agree reasonably well with the results from the more rigorous microscopic Monte Carlo method. For a full gas-grain model, H atom encounter desorption can reduce surface H abundances. Therefore, if a model adopts the encounter desorption of H atoms, it becomes more difficult for hydrogenation products such as methanol to form, but it is easier for C, O and N atoms to bond with each other on grain surfaces.

Key words: astrochemistry-ISM: abundances-ISM: molecules-ISM

1 INTRODUCTION

The grain ice mantle is observed to be mainly composed of water ice (Öberg et al. 2011), thus, the substrate for the grain-surface chemical reactions is usually assumed to be water ice only in the traditional astrochemical models (Hasegawa et al. 1992; Hasegawa & Herbst 1993; Garrod & Herbst 2006). However, this assumption may not be valid if the grain ice mantle is composed of other surface species on which the desorption energies of surface species differ significantly from these on water ice. For instance, the desorption energy of surface species on H₂ substrate is more than one order of magnitude lower than that on water ice (Cuppen & Herbst 2007). If we still assume the substrates are water ice only, hydrogen molecules may be depleted in the gas phase and are frozen on grains at low temperatures and high densities (Hincelin et al. 2015). However, to the best of our knowledge, the depletion of H₂ has never been reported. So, for better astrochemical modeling, there should be at least two kinds of substrates on grain surface, water and molecular hydrogen in a chemical model.

In order to consider the much lower desorption energy of surface species on molecular hydrogen in astrochemical models, Morata & Hasegawa (2013) made a crude approximation and assumed that the dust grains are completely covered by H₂ at 10 K. However, to the best of our knowledge, the validity

of this assumption has not been proved. [Garrod & Pauly \(2011\)](#) suggested another approach to solve the problem. They used the fractional coverage of surface H_2 to adjust the desorption energies on water ice in their models. The adjusted desorption energies are named the effective binding energies. One major limitation of this approach is that an empirical modifying factor has to be used to calculate the effective binding energies.

It is straightforward to include both H_2 and water ice substrates in the microscopic Monte Carlo (MC) models ([Chang et al. 2005](#); [Cuppen et al. 2017](#)). This numerical approach keeps track of the trajectory of each surface species when it hops among binding sites. If a surface species hops into a site where there is one H_2 molecule, the substrate for that surface species is H_2 ice. Otherwise, the substrate is water ice. However, this numerical approach is computationally expensive when the surface temperatures are high (≥ 15 K) because the hopping events of surface species consume most CPU time at high temperatures. Therefore, so far this approach can only be used to simulate the chemistry of cold sources such as the dark molecular clouds.

Recently, a new mechanism called the encounter desorption was suggested so that surface H_2 abundances on heterogeneous grain surface can be calculated by the rate equation (RE) approach ([Hincelin et al. 2015](#)). This mechanism considers the desorption of hydrogen molecules when they encounter other surface H_2 molecules. The implementation of this mechanism in astrochemical models is very convenient. Only one extra surface reaction $gH_2 + gH_2 \rightarrow H_2 + gH_2$ has to be added into the chemical reaction network, where the letter g designates surface species. Moreover, the rate coefficient of the extra surface reaction has a simple analytical formula ([Hincelin et al. 2015](#)). The calculated surface H_2 abundances by the rate equation approach from models including this reaction agree reasonably well with the results calculated by the microscopic MC method.

Hydrogen atoms can diffuse almost as fast as gH_2 on grain surface, so they should encounter H_2 frequently on grain surfaces if gH_2 is abundant. The desorption energy of H atoms on gH_2 substrates is about 45 K ([Cuppen & Herbst 2007](#)), so H atoms should sublime quickly when they encounter gH_2 molecules just like molecular hydrogen. Because the surface chemistry is dominated by hydrogenation reactions when the grain temperature is around 10 K, grain surface chemistry is likely to be affected if the encounter desorption of H atoms is included in models.

In this work, we investigate how grain surface chemistry are affected by the encounter desorption of H atoms. The paper is organized as follows. In Section 2, we derive math formula for the rate coefficient of H atom encounter desorption on grain surface. In Section 3, we show that for a simple reaction network that include the encounter desorption of H atoms, the surface H abundances calculated by the rate equation approach agree reasonably well with those predicted by the microscopic MC approach. In Section 4, we simulate a full gas-grain reaction network that includes the encounter desorption of gH_2 molecules and gH atoms and present the impacts of gH atoms encounter desorption on the surface chemistry in cold cores. In Section 5, we summarize our findings and draw the conclusions.

2 THE ENCOUNTER DESORPTION OF H SURFACE ATOMS

Following the gH_2 encounter desorption mechanism, in order to include the gH encounter desorption mechanism in a chemical model, we can simply add an extra reaction, $gH + gH_2 \rightarrow H + gH_2$, to the chemical reaction network. Before deriving the rate coefficient for this reaction, we first review the encounter desorption mechanism of gH_2 and derive the rate coefficient for the reaction $gH_2 + gH_2 \rightarrow H_2 + gH_2$.

[Figure 1](#) shows the diffusion of gH_2 on a heterogeneous ice mantle composed of water ice and H_2 . We assume that the ice mantle is mainly composed of water ice, which agrees with observations toward cold sources ([Öberg et al. 2011](#)). When a hydrogen molecule hops from a water ice binding site to another site that is occupied by gH_2 as shown in the figure, gH_2 desorption competes with the hopping events of gH_2 . The probability that gH_2 desorbs is given by the following equation ([Chang et al. 2005](#)),

$$P_{H_2} = \frac{b_{H_2H_2}}{b_{H_2H_2} + k_{H_2H_2}}, \quad (1)$$

where $b_{H_2H_2}$ and $k_{H_2H_2}$ are the thermal desorption and hopping rates of gH₂ on gH₂ substrates respectively. The thermal desorption rate of gH₂ on gH₂ substrates is, $b_{H_2H_2} = \nu \exp(-E_{D_{H_2H_2}}/T)$ while the hopping rate of gH₂ on gH₂ substrates is, $k_{H_2H_2} = \nu \exp(-E_{b_{H_2H_2}}/T)$, where $E_{D_{H_2H_2}}$ and $E_{b_{H_2H_2}}$ are desorption energy and diffusion barrier of gH₂ on gH₂ substrates. Assuming the number of binding sites occupied by gH₂ is much smaller than the total number of binding sites on the grain surface, the rate coefficient for two hydrogen molecules to encounter is given by,

$$r_{H_2H_2} = \frac{2k_{H_2H_2O}}{S}, \quad (2)$$

where $k_{H_2H_2O}$ is the hopping rate of gH₂ on water ice while S is the total number of binding sites on the grain surface. Similarly, $k_{H_2H_2O} = \nu \exp(-E_{b_{H_2H_2O}}/T)$, where $E_{b_{H_2H_2O}}$ is the diffusion barrier of gH₂ on water ice. Finally, we have the rate coefficient for the reaction $gH_2 + gH_2 \rightarrow H_2 + gH_2$, which has a simple analytical form,

$$r_{enc_{H_2}} = r_{H_2H_2} P_{H_2}. \quad (3)$$

Figure 1 also shows the diffusion of gH on grain ice mantle and the encounter of gH and gH₂. The rate coefficient for the reaction $gH + gH_2 \rightarrow H + gH_2$, $r_{enc_{HH_2}}$ can be derived as the follows. First, the probability that a gH atom desorbs into the gas phase after it encounters a gH₂ molecule is,

$$P_{HH_2} = \frac{b_{HH_2}}{b_{HH_2} + k_{HH_2}}, \quad (4)$$

where $b_{HH_2} = \nu \exp(-E_{D_{HH_2}}/T)$ and $k_{HH_2} = \nu \exp(-E_{b_{HH_2}}/T)$ are the thermal desorption and hopping rates of gH on gH₂ substrates respectively. The two parameters $E_{D_{HH_2}}$ and $E_{b_{HH_2}}$ are the desorption energy and diffusion barrier of gH on gH₂ respectively. The gH and gH₂ encounter rate coefficient is,

$$r_{HH_2} = \frac{k_{H_2H_2O} + k_{HH_2O}}{S}, \quad (5)$$

where k_{HH_2O} is the hopping rate of gH on water ice, which is dependent on the diffusion barrier of gH on water ice, $k_{HH_2O} = \nu \exp(-E_{b_{HH_2O}}/T)$. There are two possible scenarios that hydrogen atoms encounter hydrogen molecules. Either a gH atom hops into a site already occupied by gH₂ or vice versa. The encounter desorption of gH only occurs in the first case. We will explain the reason in the next section, where the microscopic MC method will be briefly introduced. The probability for the first case to occur is, $P = \frac{k_{HH_2O}}{k_{H_2H_2O} + k_{HH_2O}}$. Finally we have,

$$\begin{aligned} r_{enc_{HH_2}} &= r_{HH_2} P P_{HH_2} \\ &= \frac{k_{HH_2O} b_{HH_2}}{S(b_{HH_2} + k_{HH_2})} \end{aligned} \quad (6)$$

Here we only consider thermal desorption in the above derivation. If other desorption mechanism such as photodesorption is included in the models (Öberg et al. 2007), we can show that the rate coefficient for gH encounter desorption is,

$$r_{enc_{HH_2}} = \frac{k_{HH_2O} (\sum_i b_{iHH_2})}{S(\sum_i b_{iHH_2} + k_{HH_2})}, \quad (7)$$

where $\sum_i b_{iHH_2}$ are the sum of the rates of all possible desorption mechanisms for gH on gH₂ substrates.

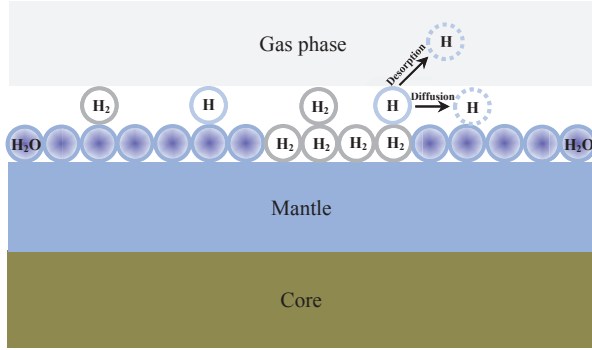


Fig. 1: The diffusion of gH_2 and gH on substrates covered by water and gH_2 and the encounter desorption of gH .

3 NUMERICAL COMPARISON

In order to test the validity of H atoms encounter desorption mechanism, we compare results from RE models with the inclusion of gH and gH_2 encounter desorption mechanism (hereafter REED) with these calculated by the microscopic MC approach. However, so far it is not possible to simulate a chemical model that include H_2 accretion for any meaningful length of time using the microscopic MC method because the H_2 accretion and gH_2 hopping consume too much CPU time. Therefore, following [Hincelin et al. \(2015\)](#), we can only compare the steady-state gH abundances calculated by these two approaches. Moreover, we also adopt a simple chemical model which only consider the accretion of H and H_2 , the thermal and encounter desorption of gH and gH_2 and the recombination of gH atoms on grain surfaces to form gH_2 .

We adopt a typical dust grain with radius $0.1 \mu\text{m}$. A such grain has $S = 10^6$ binding sites. The desorption energies of gH_2 on water ice and gH_2 are assumed to be 440 K ([Hincelin et al. 2015](#)) and 23 K ([Cuppen & Herbst 2007](#)) respectively while the desorption energy of gH on water ice and gH_2 are assumed to be 450 K ([Garrod & Herbst 2006](#)) and 45 K ([Cuppen & Herbst 2007](#)) respectively. The diffusion barriers are always set to be half of the desorption energy for all surface species. Both the gas and dust temperatures are assumed to 10 K in our simulations. We assume the density of H_2 to be constant in each simulation. We perform simulations using a wide range of H nuclei densities, which vary from $2 \times 10^4 \text{ cm}^{-3}$ to $2 \times 10^{14} \text{ cm}^{-3}$. Because the fractional abundance of H is around 1.0×10^{-4} in dense clouds ([Chang et al. 2007](#)), we assume the fractional abundance of H atoms is fixed to be $\frac{\sqrt{2}}{4} \times 10^{-4}$ for all H nuclei densities for simplicity. So, the accretion rate of H atom is,

$$k_{accH}X(H) = 1.0 \times 10^{-4}k_{accH_2}X(H_2), \quad (8)$$

where k_{accH_2} and k_{accH} are the accretion rate coefficients of gas-phase H_2 and H respectively while $X(H_2)$ and $X(H)$ are the densities of these two species respectively. Moreover, in order for a preliminary study of the effect of the gH encounter desorption on the surface chemistry, we also use the RE approach to calculate another chemical model which has all the above reactions other than the encounter desorption of gH atoms. Hereafter, this model is called REED2 model.

We briefly introduce the microscopic MC approach as the follows and refer to [Chang et al. \(2005\)](#) for details of this numerical method. Grain surface binding sites form a $L \times L$ square lattice, where $L = \sqrt{S}$. When gas-phase species accrete on grains, they are randomly located into binding sites. At time t , a surface species gI either hop to a neighboring site or desorb after a waiting time,

$$\delta t = -\ln(X)/(b_I(t) + k_I(t)), \quad (9)$$

where $b_I(t)$ and $k_I(t)$ are the desorption and hopping rates of species I at the time t respectively while X is random number uniformly distributed within $(0, 1)$. If the site where species I resides at the time t is already occupied by gH_2 , the value of $b_I(t)$ should be the desorption rate of the species I on gH_2 . Otherwise, it is the desorption rate of species I on water ice. Similarly, the value of $k_I(t)$ depends on whether the binding site is occupied by gH_2 or not. The species I hops into a neighboring site if $k_I(t) \geq Y(b_I(t) + k_I(t))$, where Y is another random number uniformly distributed within $(0, 1)$. Otherwise it will desorb. A chemical reaction occurs if the species I hops into a site and encounters a reactive species.

In the microscopic MC simulations, the initial gH and gH_2 abundances are zero. As H and H_2 accrete on the grain surface, gH abundance initially increases and then fluctuates around its mean value after the steady-state has been reached. The average abundance of gH between time t_0 and t_1 , which are both after the steady-state has been reached, is,

$$g\bar{H}(t_0, t_1) = \frac{\sum_i i \Delta t_i}{t_1 - t_0}, \quad (10)$$

where Δt_i is the time interval during which the number of gH atoms is i and $\sum_i \Delta t_i = t_1 - t_0$. If $t_1 - t_0$ is sufficiently large, $g\bar{H}$ converges to a value that is independent on t_1 , t_0 nor $t_1 - t_0$. At the low H nuclei density ($\sim 10^{-6} \text{ cm}^{-3}$), $t_1 - t_0$ is a time period during which about 4000 H atoms accrete on grain surface so that $g\bar{H}$ can converge. As the H nuclei densities increase, more H atoms are required to accrete during the time period $t_1 - t_0$ so that $g\bar{H}$ converges because of the larger gH population fluctuations. We use the converged $g\bar{H}$ values to compare with the abundances of gH predicted by RE approach.

As introduced earlier, hydrogen atoms can encounter gH_2 in two different ways. When a gH atom hops into a site occupied by gH_2 , the desorption and hopping rates of gH significantly increase because of the significantly reduced desorption energy and diffusion barrier of gH on gH_2 . On the other hand, when a gH_2 molecule hops into a water binding site occupied by a gH atom, the gH atom cannot hop or desorb until the gH_2 molecule leaves the binding site in the microscopic MC simulations (Chang et al. 2007). After the gH_2 leaves the binding site, the gH atom can hop or desorb, but its desorption energy and diffusion barrier are still these on water substrates. Therefore, the first scenario of gH_2 and gH encounter must occur so that gH desorb more quickly. If the second scenario occurs, gH_2 may also desorb more quickly on that site than on water ice because the desorption energy of gH_2 on gH is much less than that on water ice (Cuppen & Herbst 2007). A surface reaction $\text{gH} + \text{gH}_2 \rightarrow \text{gH} + \text{H}_2$ can be included in the reaction network in the RE approach in order to take into account of this gH_2 molecules desorption process when they encounter gH atoms. However, because gH_2 is much more abundant than gH , this event occurs much less frequently than the process gH_2 encounter other hydrogen molecules does. Therefore, in this work, we ignore this desorption process and assume that the desorption energy of gH_2 on gH is the same as that on water ice. Thus, the reaction $\text{gH} + \text{gH}_2 \rightarrow \text{gH} + \text{H}_2$ is not included in the reaction network.

Figure 2 shows the steady-state gH abundance as a function of H_2 density from the microscopic MC and REED models. It can be seen that the gH abundances predicted by the REED models agree very well with the results from the microscopic MC model for a wide range of H_2 density between 10^4 cm^{-3} and 10^{12} cm^{-3} . At the density of 10^4 cm^{-3} , gH abundance predicted by the microscopic MC method is slightly higher than that from the REED model because of the ‘‘back diffusion’’ problem. When the abundances of reactive surface species are very low on grain surface, two species must visit around 3S binding sites in order to encounter each other (Lohmar & Krug 2006; Chang et al. 2006). So the reaction rates in the RE model are over estimated while the microscopic MC method already takes into account the back diffusion. At higher H_2 densities, surface H_2 density also increases so that the back diffusion problem becomes less significant (Chang et al. 2006). Thus, the REED model results agree better with the microscopic MC model results. However when the H_2 density is above 10^{13} cm^{-3} , the microscopic MC model predicts that hydrogen molecules occupy about 70 percent of the total number of grain surface binding sites (Hincelin et al. 2015). If gH hops from one binding site to another, it is very likely that the second binding site is also occupied by gH_2 . This possibility is not considered by the

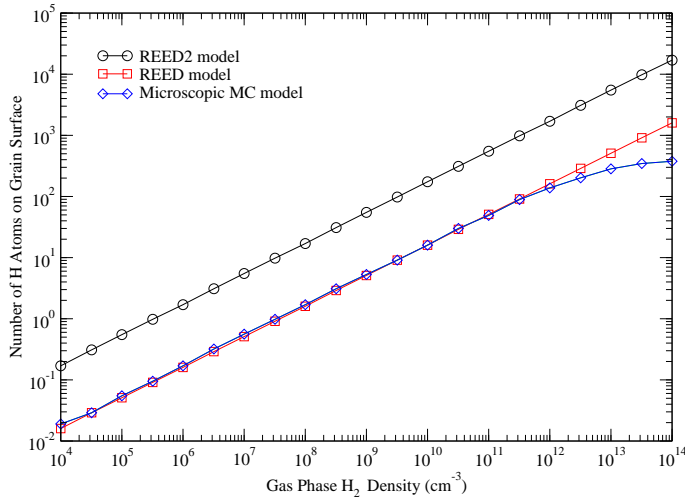


Fig. 2: The steady-state surface H atom abundances with respect to H_2 density predicted by the REED, REED2 and microscopic MC models using a simple chemical reaction network.

RE approach. Therefore, the discrepancy between the REED and microscopic model results increase as gas-phase H_2 abundance increases. At the highest H_2 density, the abundance of gH from the REED model is about a factor of four larger than that from the microscopic MC model.

Figure 2 also shows the steady-state gH abundance as a function of H_2 density for the REED2 model. We can see that the gH encounter desorption mechanism can decrease gH abundance by about one order of magnitude for the simple reaction network. Grain surface reactions are dominated by hydrogenation reactions at 10 K, so the significant decrease of gH abundance may change the abundances of icy species in a much larger gas-grain chemical model. The effects of gH encounter desorption on the formation of surface species at 10 K in a larger chemical model will be presented in the next section.

We fix the fractional abundance of H atoms to be $\frac{\sqrt{2}}{4} \times 10^{-4}$ in the above simulations, however, the fractional abundances of H atoms in astronomical sources may not be always around that value. In order to study how the fractional abundances of H may affect the validity of H atoms encounter desorption mechanism, we fix the H nuclei density to be $2 \times 10^6 \text{ cm}^{-3}$ and simulate the REED and microscopic MC models using a wide range of H fractional abundances, which vary from 10^{-6} to 0.1. We found that the gH abundances predicted by the REED model fall within 50 percent of that by the microscopic MC model over the wide range of H fractional abundances. Therefore, the agreement of the REED model with the microscopic MC model results is not likely to be noticeably affected by the fractional abundance of H atoms.

4 EFFECTS OF H ATOMS ENCOUNTER DESORPTION ON THE COLD CORE CHEMISTRY

The encounter desorption mechanism is not likely to be important when grain temperatures are high enough so that almost all gH_2 molecules sublime because the encounter events would be few if gH_2 abundance is low. Therefore, we only study the effects of H atoms encounter desorption on cold core chemistry.

The full gas-grain chemical reaction network was adapted from Garrod et al. (2007) and updated based on KIDA (Hincelin et al. 2011), which has 654 species and 6210 chemical reactions. The reactive desorption mechanism is included in this reaction network. Its coefficient is set to be 0.01. Initially, all species are assumed to be in the gas phase. The initial low-metal elemental abundances are taken from Semenov et al. (2010). The effect of quantum tunneling for grain-surface species is not considered in this work (Katz et al. 1999). The two-phase model is used in all simulations. We use a standard dust

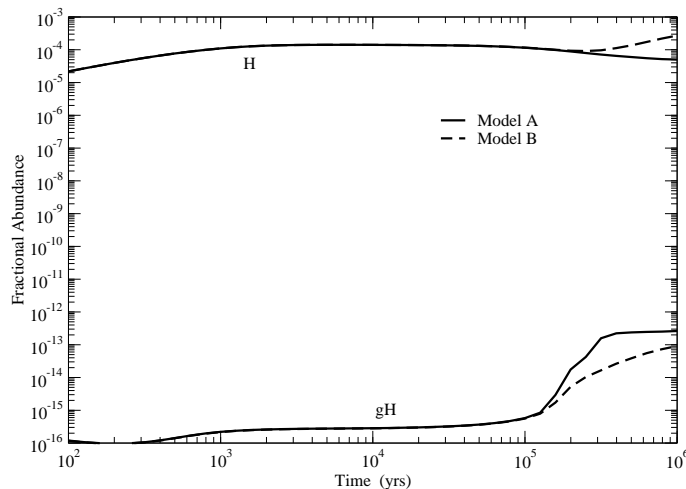


Fig. 3: The gas-phase and surface H atom abundances as a function of time in models A and B.

grain with radius $0.1 \mu\text{m}$ with surface binding site density $1.5 \times 10^{15} \text{ cm}^{-2}$. Both the grain and gas phase temperatures are set to 10 K and the density of H nuclei is $2 \times 10^4 \text{ cm}^{-3}$ in our models. The cosmic-ray ionization rate is $1.3 \times 10^{-17} \text{ s}^{-1}$ and the visual extinction is 10 mag. Similar to the simple reaction network discussed above, the desorption energies of gH on water ice and gH₂ are 450 K and 45 K respectively while the desorption energies of gH₂ on water ice and gH₂ are 440 and 23 K respectively. The ratio of the diffusion barrier of each surface species to its desorption energy is kept to be 0.5 in our models.

We simulate two chemical models. Model A includes the reaction $\text{gH}_2 + \text{gH}_2 \rightarrow \text{H}_2 + \text{gH}_2$ but not the reaction $\text{gH} + \text{gH}_2 \rightarrow \text{H} + \text{gH}_2$. In model B, the two reactions $\text{gH}_2 + \text{gH}_2 \rightarrow \text{H}_2 + \text{gH}_2$ and $\text{gH} + \text{gH}_2 \rightarrow \text{H} + \text{gH}_2$ are included in its reaction network. In total, there are 6211 and 6212 chemical reactions in models A and B respectively. Both models are calculated by the OSU gas-grain rate equation codes (Garrod & Herbst 2006).

Figure 3 shows the temporal evolution of gas-phase and surface H atom abundances predicted by models A and B. Because the H atom encounter desorption mechanism is included in model B, gH abundance from model B is typically lower than from model A. It is interesting that at the time earlier than 10^5 yrs, models A and B predict similar gH and H abundances, which can be explained as the follows. At the early time, there are abundant O, C and N in the gas phase, so most gH atoms react with gO, gC and gN on grain surface instead of encountering gH₂ molecules and desorbing. When O, C and N atoms are depleted in the gas phase, it becomes more difficult for gH to find these atoms on grain surface to recombine, so gH can encounter gH₂ molecules more frequently. As a result, the impact of gH encounter desorption becomes more significant. Thus, the discrepancy between the gH abundances predicted by these two models becomes larger. At the time later than 3×10^5 yrs, however, gH abundances predicted by model B become closer to that by model A, which can be explained as the follows. In Figure 3, after 3×10^5 yrs, the gas-phase H atom abundances gradually increase with time in model B while its abundances decrease with time in model A. At the time 10^6 yrs, gas-phase H atom abundance in model B is about a factor of 4 larger than that in model A. Because of the higher gas-phase H atom density in model B, more H atoms accrete on grains in model B than in model A after the time 3×10^5 yrs. So, gH abundances in model B are closer to that in model A after the time 3×10^5 yrs. The largest discrepancy between the gH abundances predicted by these two models is about one order of magnitude, which occurs at around the time 3×10^5 yrs.

Figure 4 shows selected major surface species abundances as a function of time from models A and B. These species are all surface hydrogenated products. We can see that the production of water ice and gNH₃ are not much affected by the gH encounter desorption mechanism introduced in model

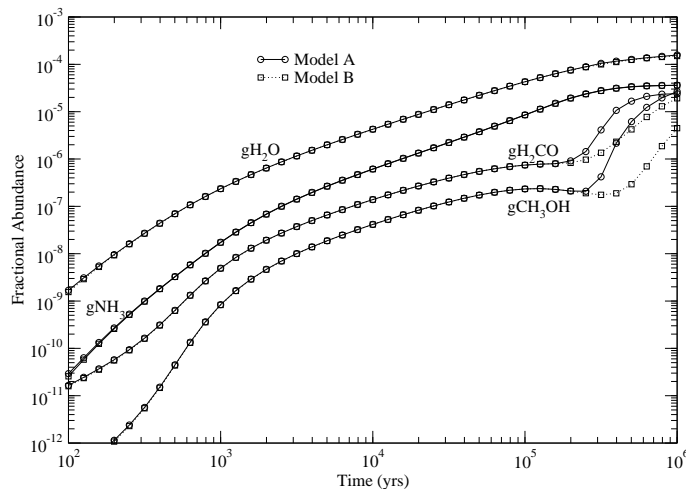


Fig. 4: The fractional abundances of selected major icy species as a function of time in models A and B.

B. However, after the time 10^5 yrs, model B predicts lower $g\text{CH}_3\text{OH}$ and $g\text{H}_2\text{CO}$ abundances than model A does because $g\text{H}$ atom abundances in model B are lower. Difference of the impact on surface species production may be explained by the reaction barriers of hydrogenation reactions. Hydrogenation reactions that form $g\text{H}_2$ and $g\text{NH}_3$ are barrierless, thus, the rate coefficients of these hydrogenation reactions are large enough so that even when the $g\text{H}$ abundances decrease, almost all $g\text{O}$ and $g\text{N}$ atoms can still be hydrogenated to form water and $g\text{NH}_3$ respectively. On the other hand, not all $g\text{CO}$ molecules can be hydrogenated because the hydrogenation reaction $g\text{H} + g\text{CO} \rightarrow g\text{HCO}$ has a barrier. So, when the encounter desorption is introduced in model B, less $g\text{CO}$ can be hydrogenated, thus, less $g\text{CH}_3\text{OH}$ and $g\text{H}_2\text{CO}$ molecules are formed in model B. We can also see that although it is more difficult to hydrogenate $g\text{H}_2\text{CO}$ to form $g\text{CH}_3\text{OH}$ in model B, overall, the $g\text{H}_2\text{CO}$ abundances are reduced by the $g\text{H}$ encounter desorption mechanism. The abundance of another major surface species $g\text{CO}$ in models A and B differ by a factor less than 3. The abundances of $g\text{CO}$ predicted by model B is always higher than that by model A after the time 10^5 yrs because it is easier to hydrogenate $g\text{CO}$ in model A due to the higher $g\text{H}$ atom abundances.

The abundances of minor surface species may be more strongly affected by the encounter desorption of $g\text{H}$. Figure 5 shows the temporal evolution of selected minor surface species abundances from models A and B. After 10^5 yrs, the abundances of these surface species from model B can be more than one order of magnitude higher than the results from model A. The encounter desorption of $g\text{H}$ reduces its abundance in model B, so it is more likely that $g\text{O}$, $g\text{N}$ and $g\text{C}$ atoms react with each other to form $-\text{O}-\text{O}-$, $-\text{C}-\text{C}-$ or $-\text{C}-\text{N}-$ chemical bonds instead of reacting with $g\text{H}$ atoms in this model. Thus, more $g\text{H}_2\text{O}_2$, $g\text{O}_3$, and $g\text{HC}_3\text{N}$ can be formed in this model than in model A.

The encounter desorption of $g\text{H}$ may also impact the abundances of gas-phase species. Figure 6 shows the temporal evolution of selected gaseous species abundances. If a gas-phase species is mainly produced in the gas phase, the $g\text{H}$ encounter desorption is unlikely to impact its abundance. For instance, HC_3N is mainly synthesized in gas phase, so its abundances predicted by models A and B are almost the same. On the other hand, methanol can hardly be produced in the gas-phase. Almost all gaseous methanol are formed via reactive desorption on grain surface. Therefore, CH_3OH abundance from model B is much lower than those from model A after the time 10^5 yrs because surface methanol can be more efficiently synthesized in model A. Both H_2O_2 and H_2CO can be formed in the gas phase and via reaction desorption on grain surfaces. So, the impact of the $g\text{H}$ encounter desorption on their abundances is less than that on methanol abundances, but more than that on HC_3N abundances.

We also performed test simulations of the above two models at a higher H nuclei density, 10^5 cm^{-3} . Similarly, model B considers the $g\text{H}$ atom encounter desorption mechanism while model A does not.

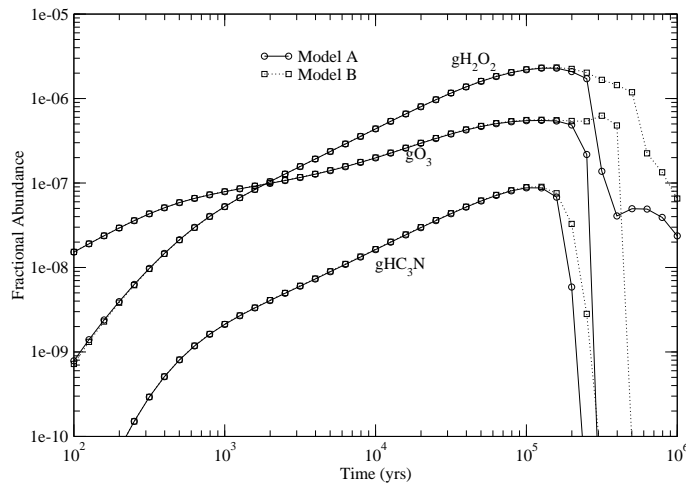


Fig. 5: The temporal evolution of the fractional abundances of selected minor icy species in models A and B.

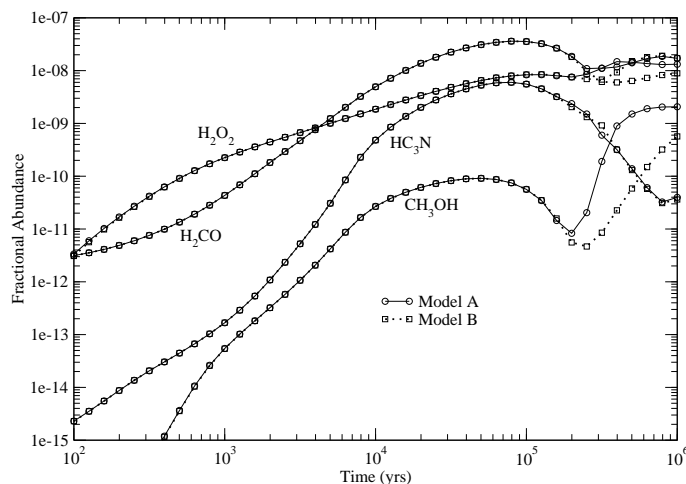


Fig. 6: The fractional abundances of selected gas-phase species as a function of time in models A and B.

We found that there are also less $g\text{CH}_3\text{OH}$ and $g\text{H}_2\text{CO}$ molecules and more surface species such as $g\text{O}_3$ in model B at the higher density. On the other hand, discrepancy between species abundances in the two models becomes less significant at the higher H nuclei density. For instance, the surface methanol abundances from the model B are no more than a factor of 5 lower than that from model A at the higher H nuclei density while the discrepancy can be as much as one order of magnitude at the lower H nuclei density. We explain the decrease of the impact of the gH encounter desorption when the H nuclei density increases as follows. At the higher H nuclei density, more species that can react with gH accrete on grain surfaces, so it is more likely that gH atoms react with other surface species instead of desorbing. So, the gH encounter desorption mechanism affects grain surface chemistry less significantly at the higher H nuclei densities.

5 CONCLUSIONS AND DISCUSSIONS

The significantly reduced desorption energy of hydrogen atoms when encountering hydrogen molecules on dust grains, namely the encounter desorption mechanism of hydrogen atoms, is investigated in this work. This process can be easily included in an astrochemical model by adding a new chemical reaction, $\text{gH} + \text{gH}_2 \rightarrow \text{H} + \text{gH}_2$ to the chemical reaction network. We derived the rate coefficient for this reaction. In order to test the validity of hydrogen atom encounter desorption mechanism, we simulated a simple chemical reaction network that includes the encounter desorption of H atoms by the RE approach and calculated the steady-state surface H atom abundances. The calculated H atom abundances agree well with those predicted by the more rigorous microscopic MC method over a wide range of gas phase H_2 and H densities. Thus, the hydrogen atom encounter desorption mechanism is a reasonable approach to take into account of the facile desorption of hydrogen atoms on substrates composed of hydrogen molecules and water ice.

We simulated two full gas-grain chemical models under standard physical conditions that pertain to dense cores to investigate the impact of gH encounter desorption mechanism. The gH encounter desorption mechanism is present in model B, but not in model A. We found that the gH atom encounter desorption can affect grain surface chemistry in two ways. Firstly, it becomes more difficult for hydrogenation reactions with barriers to fire if the gH atom encounter desorption mechanism is included in the chemical model. Thus, the abundances of surface species such as methanol drops in the model because surface reactions that produce these surface species have barriers. Secondly, gO, gN and gC atoms are more likely to react with each other instead of reacting with gH atoms in a model that includes the gH atom encounter desorption mechanism.

Our approach can be generalized to other cases in which the facile desorption of a surface species gX on a substrate gY other than water ice has to be considered. We can simply add one surface reaction, $\text{gX} + \text{gY} \rightarrow \text{X} + \text{gY}$ in the chemical reaction network. The rate coefficient for this reaction can be derived in the same way as that for gH encounter desorption.

Initially, the gH_2 encounter desorption mechanism was suggested to solve the problem that the coverage of gH_2 is too high at low temperatures and high H nuclei densities. Our study shows that at the lower H nuclei density, the gH encounter desorption mechanism may affect the production of surface species significantly. On the other hand, the major advantage of this approach is that it is very simple and easy to be implemented in a chemical model. Thus, this mechanism could be adopted widely in astrochemical modeling.

Acknowledgements We thank our referee for his/her constructive comments to improve the quality of the manuscript. The research was funded by The National Natural Science Foundation of China under grant 11673054, 11973075 and 11973099.

References

- Chang, Q., Cuppen, H. M., & Herbst, E. 2005, *A&A*, 434, 599 [2](#), [4](#)
 Chang, Q., Cuppen, H. M., & Herbst, E. 2006, *A&A*, 458, 497 [5](#)
 Chang, Q., Cuppen, H. M., & Herbst, E. 2007, *A&A*, 469, 973 [4](#), [5](#)
 Cuppen, H. M., & Herbst, E. 2007, *ApJ*, 668, 294 [1](#), [2](#), [4](#), [5](#)
 Cuppen, H. M., Walsh, C., Lamberts, T., et al. 2017, *Space Sci. Rev.*, 212, 1 [2](#)
 Garrod, R. T., & Herbst, E. 2006, *A&A*, 457, 927 [1](#), [4](#), [7](#)
 Garrod, R. T., & Pauly, T. 2011, *ApJ*, 735, 15 [2](#)
 Garrod, R. T., Wakelam, V., & Herbst, E. 2007, *A&A*, 467, 1103 [6](#)
 Hasegawa, T. I., & Herbst, E. 1993, *MNRAS*, 261, 83 [1](#)
 Hasegawa, T. I., Herbst, E., & Leung, C. M. 1992, *ApJS*, 82, 167 [1](#)
 Hincelin, U., Chang, Q., & Herbst, E. 2015, *A&A*, 574, A24 [1](#), [2](#), [4](#), [5](#)
 Hincelin, U., Wakelam, V., Hersant, F., et al. 2011, *A&A*, 530, A61 [6](#)
 Katz, N., Furman, I., Biham, O., Pirronello, V., & Vidali, G. 1999, *ApJ*, 522, 305 [6](#)
 Lohmar, I., & Krug, J. 2006, *MNRAS*, 370, 1025 [5](#)

- Morata, O., & Hasegawa, T. I. 2013, MNRAS, 429, 3578 [1](#)
- Öberg, K. I., Boogert, A. C. A., Pontoppidan, K. M., et al. 2011, ApJ, 740, 109 [1](#), [2](#)
- Öberg, K. I., Fuchs, G. W., Awad, Z., et al. 2007, ApJ, 662, L23 [3](#)
- Semenov, D., Hersant, F., Wakelam, V., et al. 2010, A&A, 522, A42 [6](#)